

Four-Unit-Cell Superstructure in the Optimally Doped $\text{YBa}_2\text{Cu}_3\text{O}_{6.92}$ Superconductor

Zahirul Islam,^{1,*} X. Liu,² S. K. Sinha,² J. C. Lang,¹ S. C. Moss,³ D. Haskel,¹ G. Srajer,¹ P. Wochner,⁴ D. R. Lee,¹
D. R. Haefner,¹ and U. Welp⁵

¹*Advanced Photon Source, Argonne National Laboratory, Argonne, Illinois 60439, USA*

²*Department of Physics, University of California, San Diego, California 92093, USA*

³*Department of Physics and Texas Center for Superconductivity and Advanced Materials, University of Houston, Houston, Texas 77204, USA*

⁴*Max-Planck-Institut für Metallforschung, 70569 Stuttgart, Germany*

⁵*Materials Science Division, Argonne National Laboratory, Argonne, Illinois 60439, USA*

(Received 23 December 2003; published 7 October 2004)

Diffuse x-ray scattering measurements reveal that the optimally doped $\text{YBa}_2\text{Cu}_3\text{O}_{6.92}$ superconductor is intrinsically modulated due to the formation of a kinetically limited 4-unit-cell superlattice, $\mathbf{q}_0 = (\frac{1}{4}, 0, 0)$, along the shorter Cu-Cu bonds. The superlattice consists of large anisotropic displacements of Cu, Ba, and O atoms, respectively, which are correlated over ~ 3 – 6 unit cells in the ab plane, and appears to be consistent with the presence of an O-ordered “ortho-IV” phase. Long-range strains emanating from these modulated regions generate an inhomogeneous lattice which may play a fundamentally important role in the electronic properties of yttrium-barium-copper-oxides.

DOI: 10.1103/PhysRevLett.93.157008

PACS numbers: 74.72.Bk, 61.10.Eq, 74.25.-q

There is mounting evidence that the cuprate superconductors are intrinsically inhomogeneous, even in the superconducting (SC) phase. The driving force for such inhomogeneities may well be electronic instabilities [1], or elastic strain [2], or a combination of these. Furthermore, in the case of the $\text{YBa}_2\text{Cu}_3\text{O}_{6+x}$ (YBCO) system, the oxygen vacancies in the Cu-O chains tend to form superstructures which order [3] well above the SC transition temperatures according to the scheme proposed by de Fontaine and co-workers [4]. In this Letter, we describe diffuse x-ray scattering data which yield a quantitative description of how large-amplitude atomic displacements modulated with a 4-unit-cell periodicity ($\mathbf{q}_0 = (\frac{1}{4}, 0, 0)$) form coherent regions of kinetically limited imperfect order in the optimally doped $\text{YBa}_2\text{Cu}_3\text{O}_{6.92}$ superconductor. Long-range strain fields emanating from these regions create an intrinsically inhomogeneous lattice which manifests itself below ~ 200 K due to the reduction in the thermal diffuse scattering (TDS). These properties persist in the SC phase and appear to be universal to the YBCO compounds [5]. These findings are of great importance in several respects. Theoretical work [2] has shown how inhomogeneous electronic phases on different length scales can arise due to elasticity-driven lattice deformations, and how such deformations can suppress superconductivity and modulate the electronic density of states. Furthermore, locally modulated regions can act as resonant electron scattering centers, affecting transport and susceptibility properties [6], while strains, as in the twin boundaries, can pin vortices [7]. According to other theoretical work [8], dopants or vacancies may locally nucleate highly anharmonic lattice modulations around them (“breather modes”) which can affect the SC order parameter. Thus, a treatment of the superconductivity in terms of a

single homogeneous phase in these materials appears somewhat unrealistic.

We have previously found in an underdoped YBCO ($x \approx 0.63$) compound short-range ordered superstructures [5] with a periodicity, $\mathbf{q}_0 = (\sim \frac{2}{5}, 0, 0)$, coincident with a harmonic of the so-called “ortho-V” phase of O-vacancy ordering on the Cu-O chains [4]. However, the intensities of the diffuse satellites clearly showed that displacements of atoms in the Cu-O chain planes, the CuO_2 planes, and the BaO planes were involved [5]. Here we show that at optimal doping, short-range ordered modulated regions, $\mathbf{q}_0 = (\frac{1}{4}, 0, 0)$, involving correlated displacements of atoms (Fig. 1), indeed coexist with superconductivity. Identical modulations were also observed in a twinned crystal [5]. Since the data in the detwinned crystal are not complicated by contributions from twin domains, we focus on the detwinned crystal in this Letter.

For this study, a high-quality *detwinned* crystal ($\sim 1 \text{ mm} \times 1 \text{ mm} \times 130 \mu\text{m}$) of optimally doped YBCO ($T_c = 91.5 \text{ K}$, $\Delta T_c \approx 1 \text{ K}$) was chosen. The crystal was annealed at 420°C in flowing pure O_2 for about a week and was stress detwinned in flowing O_2 at the same temperature. Polarization-sensitive optical microscopy showed the presence of a single twin domain. The crystal mosaic was $\sim 0.03^\circ$. The c axis was perpendicular to the large crystal facet. High-energy (36 keV) x-ray diffraction studies were performed on the 4ID-D beam line at the Advanced Photon Source. Experimental details can be found elsewhere [5].

Figures 2(a)–2(d) show several \mathbf{a} -axis H -scans normal to the Cu-O-Cu chain direction for different integer values of K taken at $\sim 7 \text{ K}$. Broad satellite peaks in the diffuse scattering corresponding to $\mathbf{q}_0 = (\frac{1}{4}, 0, 0)$ are clearly visible near Bragg peaks $(h, k, 0)$: when h and k have mixed parity, the structure factor including TDS is

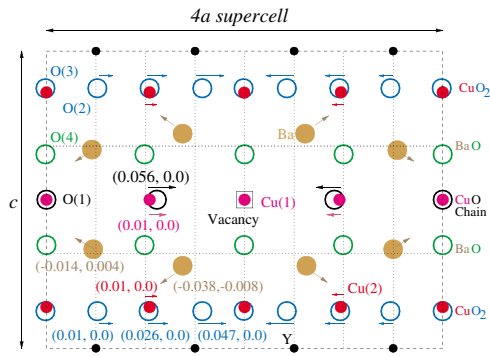


FIG. 1 (color). An ideal atomic displacement (arrows) pattern at ~ 7 K. All the atoms have been projected on the ac plane. Note that primary displacements ($\delta\mathbf{u}$'s) are along the \mathbf{a} axis, *i.e.*, along the shorter Cu-Cu bond direction. $\delta\mathbf{u}$'s, (δ_a, δ_c) in units of a and c , of respective atoms are given in parentheses. $\delta\mathbf{u}$'s of all other atoms are related by mirror symmetry.

weak. The intensity of the peak at $\mathbf{Q} = \mathbf{G} + \mathbf{q}_0$ (\mathbf{G} is a reciprocal lattice vector) is some $\sim 10^6$ orders of magnitude weaker than that of the $(4, 0, 0)$ Bragg peak. The width in the \mathbf{a}^* direction of \mathbf{q}_0 satellites is much larger than the resolution, indicating a very short correlation range ($\xi_a \sim 3a$, using Scherrer formula [9]) along the \mathbf{a}

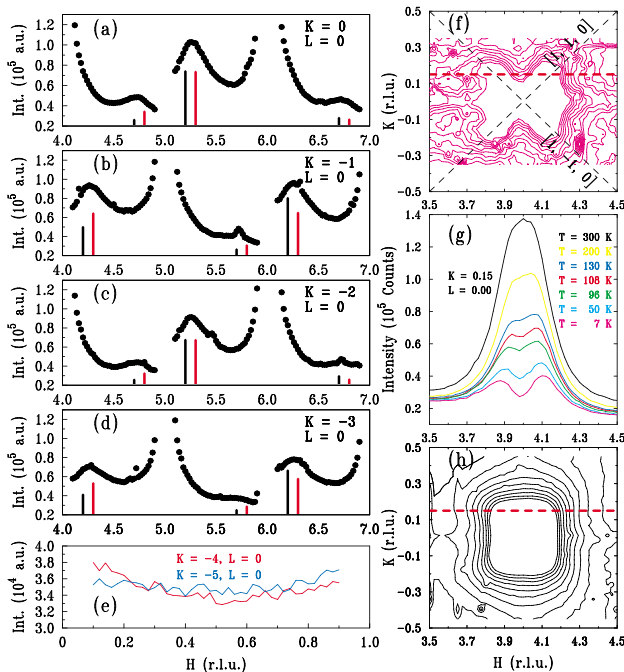


FIG. 2 (color). (a)-(d) H -scans for several integer values of K and $L = 0$. Satellite peaks are due to $\mathbf{q}_0 = (\frac{1}{4}, 0, 0)$. Vertical lines (displaced along H for clarity) compare the observed (black) and calculated (red) intensities corrected for geometric factors; (e) H -scans with high values (odd/even) of K relative to H ; (f) Contours of diffuse intensity at 7 K around $(4, 0, 0)$ Bragg peak; (g) Line scans at different T showing how TDS overwhelms HDS above ~ 200 K; (h) Contours of diffuse intensity at 300 K. Line scans in (g) were taken along the red line in (f) and (h).

axis. The use of a detwinned crystal made it unambiguous that the modulation vector is $\mathbf{q}_0 = (\frac{1}{4}, 0, 0)$ and *not* $(0, \frac{1}{4}, 0)$. The width in the \mathbf{b} -axis direction [Fig. 3(b)] corresponds to longer correlation length ($\xi_b \sim 6b$), while modulations of the intensity which extend along the \mathbf{c}^* axis through the satellite peak as shown in Fig. 3(c) indicate correlations only between neighboring Cu-O chain planes, BaO planes, and CuO_2 planes (Fig. 1), respectively, as obtained from Fourier transform (Patterson function) of these intensity patterns (similar to the results found in the underdoped systems [5]).

In addition, significant lattice-strain effects are present in this material. A 2-dimensional scan around $(4, 0, 0)$, as shown in Fig. 2(f), reveals a strongly anisotropic “bow-tie”-shape Huang diffuse scattering (HDS) pattern, with lobes extending along the four $[\pm 1, \pm 1, 0]$ directions, which require the existence of long-range strain fields generated by the modulated regions. The two superlattice peaks at $(4 \pm \frac{1}{4}, 0, 0)$ are barely discernible. A set of line scans through the diffuse lobes at several temperatures is shown in Fig. 2(g). Whereas at low T two broad peaks corresponding to two lobes are clearly visible, on increasing T the peaks become indiscernible from the rapidly growing TDS above ~ 200 K. The room-temperature diffuse scattering [Fig. 2(h)] is nearly identical to the calculated TDS (not shown) around $(4, 0, 0)$. Earlier x-ray studies [10] of tetragonal system $\text{YBa}_2(\text{Cu}_{0.955}\text{Al}_{0.045})_3\text{O}_7$ showed that HDS arises from shear distortions due to long-wave fluctuations of O concentrations in the chains along the \mathbf{a} and \mathbf{b} axes. It is possible that the O stoichi-

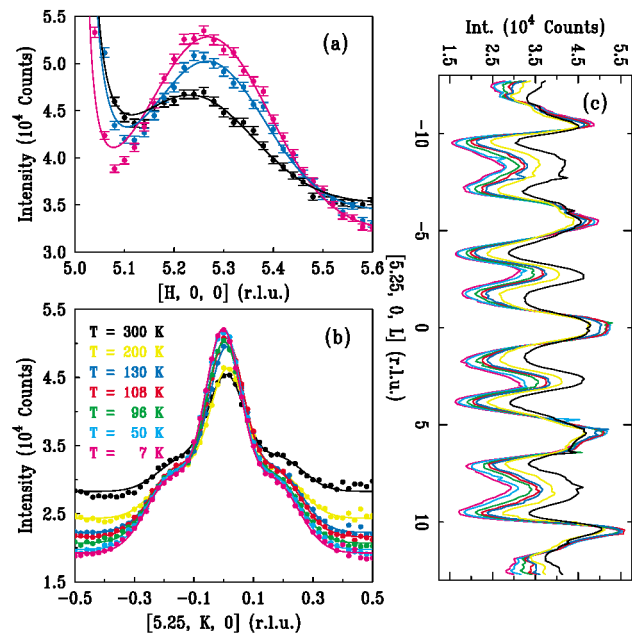


FIG. 3 (color). (a) H -scans at several temperatures. (b) K -scans through the $(5.25, 0, 0)$ peak. Lines in (a) and (b) are fits (see text). (c) Intensity modulations along \mathbf{c}^* of the same peak. Note that the oscillation amplitude grows on decreasing T . Different T 's are shown with unique colors (b).

ometry in the Cu-O chains is nonuniform in the defective short-range O-ordered domains discussed below. We note that similar HDS is also observed in optimally doped and underdoped twinned compounds eliminating the possibility that the HDS is due to stress detwinning of the crystal [5].

A 4-unit-cell periodic (ortho-IV) phase is expected near O stoichiometry of 6.75 [4] (*i.e.*, one out of every four Cu-O chains has no O atoms denoted by $\langle 1101 \rangle$) whereas in optimally doped material, the stoichiometry is 6.92 (*i.e.*, approximately one out of 12 Cu-O chains has vacancies). There are two ways to explain the formation of $\langle 1101 \rangle$ structure near optimum doping. If the O concentration is nonuniform within the Cu-O-chain planes, then vacancies tend to phase separate within the formation range of the ortho-IV phase [4]. Secondly, if the long-range Coulomb interactions among distant-neighbor vacancies are not negligible, then the $\langle 1101 \rangle$ phase can be stable even near the optimal doping with a dilute concentration of vacancies. In both cases, however, the ordering will be short ranged and imperfect, leading to significant lattice strains responsible for HDS.

Next, we note some general features of our data which were used to narrow down possible models of atomic displacements ($\delta\mathbf{u}$'s). First, a strong intensity asymmetry between the $+\mathbf{q}_0$ and $-\mathbf{q}_0$ satellites is observed around all Bragg points. A strong asymmetry can occur if $\delta\mathbf{u}$'s are large [11], or as a result of destructive interference between diffuse scattering due to disorder and displacive modulation [12] as found in quasi-1D charge density wave systems [13,14]. Second, for a given satellite at $(h, k, 0) + \mathbf{q}_0$ the intensity is either weak or very strong when h and k have the same or mixed parity, respectively. This implies out-of-phase displacements of the dominant scatterers. Third, no second harmonic ($2\mathbf{q}_0$) satellites were observed, indicating essentially a sinusoidal modulation. Finally, scans [Fig. 2(e)] such as $[H, -5, 0]$ ($H \in [0.1 - 0.9]$) found no superlattice peaks suggesting the absence of any $\delta\mathbf{u} \parallel \mathbf{b}$ associated with the \mathbf{q}_0 modulation. We performed calculations without assuming any displacements to be small in the presence of an ortho-IV phase in the Cu-O-chain plane.

Since the satellite appears at a commensurate wave vector, we can adopt a supercell model to calculate the integrated intensity using

$$I_{\text{diffuse}}(\mathbf{Q}) \propto \left| \sum_n^{\text{Supercell}} f_n(Q) e^{-W_n(Q)} e^{-i\mathbf{Q} \cdot (\mathbf{R}_n + \delta\mathbf{u}_n)} \right|^2$$

where the displacement relative to an average lattice site (\mathbf{R}_n) of the n -th atom is $\delta\mathbf{u}_n$, $f_n(Q)$ and $e^{-W_n(Q)}$ are the form factors and Debye-Waller factors (DWFs), respectively. The expression above is for integrated intensity of the satellites regardless of peak widths. Although the extraction of intensities is difficult, since the satellites are sharper than TDS and HDS, and located away from Bragg peaks, it is possible to represent the satellites at the

lowest T using a Gaussian above some monotonic background with errors in intensities varying $\sim 15\%$ – 35% depending on background modeling. A least-squares procedure was performed taking these errors into account to fit the intensities of 45 satellite peaks and the intensity modulation of the $(5.25, 0, 0)$ peak along \mathbf{c}^* . Vertical bars in Figs. 2(a)–2(d) indicate that there is good agreement between the calculated (red) and observed (black) intensities within experimental uncertainties for the resultant model shown in Fig. 1. Like the Ba and Cu atoms, both chain (O(1)) and plane oxygen atoms (O(2) and O(3)) are displaced primarily along the \mathbf{a} axis. Although there may be small displacements along the \mathbf{c} axis as well, we are more certain of them in the case of Ba. Our error estimates are $\sim 10\%$ – 15% for Ba and Cu $\delta\mathbf{u}$'s, and $\sim 15 - 25\%$ for O atoms, respectively. While the model obtained may not be perfect, it does account for all the systematics of the data. Furthermore, it portrays a pattern of displacements similar to that of ortho-V phase in an underdoped YBCO obtained from first-principles electronic calculations [15]. In our case, however, the periodicity is $4a$ (Fig. 1).

Figure 3(a) shows H -scans through a superlattice peak at several temperatures. It is clear from these scans that as T is increased, the intensity of the \mathbf{q}_0 peak decreases relative to the TDS emanating from $(5, 0, 0)$. Intensity modulation of $(5.25, 0, 0)$ peak presented in Fig. 3(c) shows that while the mean intensity of the oscillations falls with decreasing T due to the reduction of TDS, the oscillation amplitude of every other peak about the mean grows. In order to get more quantitative information as a function of temperature we fitted [5] a combination of a Lorentzian (TDS), a Gaussian, and a constant term to the H -scans [Fig. 3(a)]. K -scans shown in Fig. 3(b) are well represented by a combination of three Gaussian line profiles and a constant term to account for the background. Note that both HDS and TDS contribute to the broad lobes. Since the peak widths and positions do not change with T , only the peak heights and the constant term (*i.e.*, four parameters all together) were needed to fit the entire data. Figure 4(a) shows the T -dependence of the fitted intensity for $(5.25, 0, 0)$ peak. Although keeping positions and widths constant may introduce some sys-

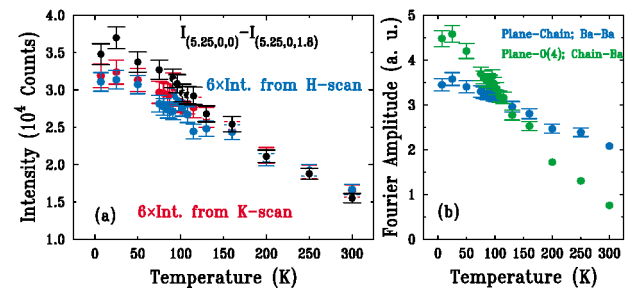


FIG. 4 (color). (a) Temperature dependence of $(5.25, 0, 0)$ peak. (b) T dependence of Fourier amplitudes obtained from intensity modulations shown in Fig. 3(c).

tematic errors for the central satellite, its integrated intensity (width \times peak intensity) agrees well with that obtained in fitting the H -scan as shown in Fig. 4(a). The intensity was also estimated via the maximum amplitude of the modulation defined as $I_{(5.25,0,0)} - I_{(5.25,0,1.8)}$. All three cases consistently show that the superlattice peak decreases nearly linearly with increasing T [Fig. 4(a)]. If this linear trend continues then the intensity will extrapolate to zero around ~ 500 K. Furthermore, Fig. 4(b) shows Fourier amplitudes obtained from intensity modulations [see Fig. 3(c)], which are a measure of displacement-displacement correlations as a function of T . It is clear that both amplitudes also grow stronger at lower temperatures.

Although the origin of \mathbf{q}_0 can be attributed to the ortho-IV phase, it is puzzling to observe a large increase of the diffuse satellite peak with decreasing T . Using the displacement model presented above and DWFs for the average lattice measured on ceramic samples [16] we estimated $\frac{I_{\text{diffuse}}(7 \text{ K})}{I_{\text{diffuse}}(300 \text{ K})} \approx 1.2$ for the intensity of (5.25, 0, 0) satellite, which is at odds with the observed ratio of at least ~ 2.2 . Since diffusive motion of chain oxygens (O(1)) practically freezes below ~ 250 K, the growth of ortho-IV regions in size or number seems unlikely. Given that atomic displacements (Fig. 1) are clearly anharmonic in these imperfectly ordered nanoscale regions, it appears that enhanced elastic softening of the lattice takes place within these regions on lowering T which may account for the low- T increase of the intensity.

To summarize, lattice modulations with a 4-unit-cell periodicity exist from above room-temperature down to the lowest temperature in optimally doped YBCO. These correspond to local regions in extent ~ 3 – 6 unit cells in the ab plane and less than one unit cell along the c axis. From the $\delta\mathbf{u}$'s (Fig. 1) one may calculate DWFs for the whole crystal and by comparison with the experimental DWFs [16], we estimate roughly $\sim 10\%$ – 20% of the crystal contain these modulated regions at the lowest T . At low temperatures clear evidence of anisotropic strain in the lattice is provided by anisotropic patterns of HDS around the Bragg points. This HDS originates with the strain induced both by the disorder between O atoms and vacancies along \mathbf{a} and \mathbf{b} axes and by the presence of modulated regions; coherent strains induced in the lattice must also exist.

Our results are suggestive when compared with the phonon anomalies and extra branches in the vicinity of $\mathbf{q}_0 = (\frac{1}{4}, 0, 0)$ observed in YBCO [17], which may arise from the modulated regions. The formation of “striped” phases and spatial modulations as those in lanthanum and bismuth-based cuprates [18,19] *per se* is insufficient to explain the diffraction effects presented in this Letter. It appears that in YBCO the electronic structure and the O vacancies together produce inherently local modulations which lead to inhomogeneous lattice and local softening within these modulated regions.

D. de Fontaine was the first to suggest the origin of \mathbf{q}_0 to be an O-ordered ortho-IV phase [4,15]. We benefitted from discussions with B.W. Veal, V. Ozolins, and D. Basov. Use of the Advanced Photon Source is supported by the U.S. Department of Energy, Office of Basic Energy Sciences, under Contract No. W-31-109-ENG-38. S. C. M. thanks the NSF for support on DMR-0099573.

*Email Address: zahir@aps.anl.gov

- [1] J. Zaanen *et al.*, Phys. Rev. B **40**, 7391 (1989); V. Emery *et al.*, Proc. Natl. Acad. Sci. U.S.A. **96**, 8814 (1999); S. A. Kivelson *et al.* Rev. Mod. Phys. **75**, 1201 (2003) and references therein; K. Machida, Physica C (Amsterdam) **158**, 192 (1989).
- [2] J.-X. Zhu *et al.*, Phys. Rev. Lett. **91**, 057004 (2003).
- [3] J. D. Jorgensen *et al.*, Phys. Rev. B **36**, 3608 (1987); R. Beyers *et al.*, Nature (London) **340**, 619 (1989); V. Plakhty *et al.*, Solid State Commun. **84**, 639 (1992); M. v. Zimmermann *et al.*, Phys. Rev. B **68**, 104515 (2003); N. H. Andersen *et al.*, Physica C (Amsterdam) **317-318**, 259 (1999).
- [4] D. de Fontaine *et al.*, Nature (London) **343**, 544 (1990); Europhys. Lett. **19**, 229 (1992); G. Ceder *et al.*, Phys. Rev. B **41**, 8698 (1990).
- [5] Z. Islam *et al.*, Phys. Rev. B **66**, 92501 (2002) and unpublished experimental work (2004).
- [6] Z. Janu *et al.*, Europhys. Lett. **64**, 399 (2003).
- [7] W. A. Caldwell *et al.*, Phys. Rev. Lett. **92**, 216105 (2004).
- [8] A. Bussmann-Holder *et al.*, J. Phys. Condens. Matter **16**, L313 (2004).
- [9] B. E. Warren, *X-Ray Diffraction* (Dover, NY 1990).
- [10] X. Jiang *et al.*, Phys. Rev. Lett. **67**, 2167 (1991); Z.-X. Cai *et al.*, Phys. Rev. B **46**, 11014 (1992).
- [11] R. W. James, *Optical Principles of the Diffraction of X-rays*, (Oxford University Press, New York, 1954), p. 565.
- [12] A. Guinier, *X-ray Diffraction in Crystals, Imperfect Crystals, and Amorphous Bodies* (W. H. Freeman and Company, San Francisco, 1963); M. A. Krivoglaz, *Theory of X-ray and Thermal-Neutron Scattering by Real Crystals* (Plenum, New York, 1969).
- [13] S. Brazovskii *et al.*, Phys. Rev. B **55**, 3426 (1997).
- [14] S. Rouzière *et al.*, Phys. Rev. B **62**, R16231 (2000).
- [15] D. de Fontaine *et al.* (to be published).
- [16] R. P. Sharma *et al.*, Physica C (Amsterdam) **174**, 409 (1991).
- [17] H. Uchiyama *et al.*, Phys. Rev. Lett. **92**, 197005 (2004); T. Egami *et al.*, Physica B (Amsterdam) **316-317**, 62 (2002); L. Pintschovius *et al.*, Phys. Rev. Lett. **89**, 37001 (2002); H. A. Mook and F. Dogan, Physica C (Amsterdam) **364-365**, 553 (2001).
- [18] J. M. Tranquada *et al.*, Nature (London) **375**, 561 (1995); Phys. Rev. B **54**, 7489 (1996); Phys. Rev. Lett. **78**, 338 (1997); M. von Zimmermann *et al.*, Europhys. Lett. **41**, 629 (1998).
- [19] J. E. Hoffmann *et al.*, Science **295**, 466 (2002); K. McElroy *et al.*, Nature (London) **422**, 592 (2003).